

# EXPERIMENTAL STUDIES ON THE WET VACUUM PUMP WITH ELMO TYPE CASING

By

Ryuichi HAYASHI\* and Osamu TORII\*\*

## 1. Introduction

The phenomena of a wet vacuum pump are very complicated because liquid and gas exist together affecting each other in the interior of the pump. Theories on a fluid machinery which deals with only liquid or gas can not be applied to a wet vacuum pump. Therefore any theoretical analysis to be satisfied has not been established yet. <sup>1),2)</sup>

Furthermore, in the experiments on a wet vacuum pump, it has been generally accepted that it is not easy to grasp the precise characteristics owing to the scattering of the measured values, and few experimental data have been published. <sup>3),4)</sup> The reason could be as follows: The characteristics of a wet vacuum pump are affected by so many factors in addition to the scale effects of the pump (e.g. gas flow rate, degree of vacuum, compression ratio, piston water\*\*\* and its supply water, etc.). Since these factors have the complicated interaction, it seems to be quite difficult to keep the experiments under control and arrange the measured values.

One of the authors has designed an accurate controlling system of the piston water for the sake of obtaining the exact and stable characteristic curves, and has already reported the experimental results on the wet vacuum pump with Nash type casing (i.e. double suction and exhaust type).

Subsequently, this paper is concerned with

\* Department of Mechanical Engineering, Faculty of Education, Shimane University, Matsue, Japan.

\*\* Department of Mechanical Engineering, Faculty of Technology, Osaka Pref. University, Osaka, Japan.

\*\*\* Because liquid acts as a piston against gas in a wet vacuum pump, it is named the piston water by the authors.

the experimental studies on the wet vacuum pump with Elmo type casing (i.e. single suction and exhaust type) and deals chiefly with the effects of the eccentricity of its casing and the flow state of piston water in the interior of the pump.

## 2. Apparatus and Experimental Methods

In Fig. 1 is drawn the general view of the experimental apparatus.

The runner 1 adopted in this experiment was the same as in Nash type casing:

outside radius :  $r_a = 100$  mm

effective width :  $b_a = 21$  mm

hub ratio :  $r_i/r_a = 0.6$

blade (straight and radial) : 16 leaves  $\times$  5 mm in thickness

Fig. 2 represents the dimensions of the suction and the exhaust port and also the measured positions of pressure in the interior of the pump. The eccentricity of Elmo type casing 2 was varied as follows:

$E (=e/r_a)$  : 0.08, 0.10, 0.12, 0.14

The capacity rate of gas flow was regulated with the suction valves. Exhaust was released in the atmosphere through the discharge pipe 7. For the measurement of the capacity rate of gas flow, two orifice flow meters 5 of 5.7 and 11.5 mm in diameter were used to be switched according to its volume.

The measurements of the degree of vacuum and pump input and the adjustment of supply water were the same as those reported in the previous paper. <sup>4)</sup> The rate of supply water was held constant (15 cc/s) during this experiment. Pump input was made comparison in terms of the net pump input subtracted a mechanical loss from the measured values, because they changed considerably corresponding to the force tightening the casing cover

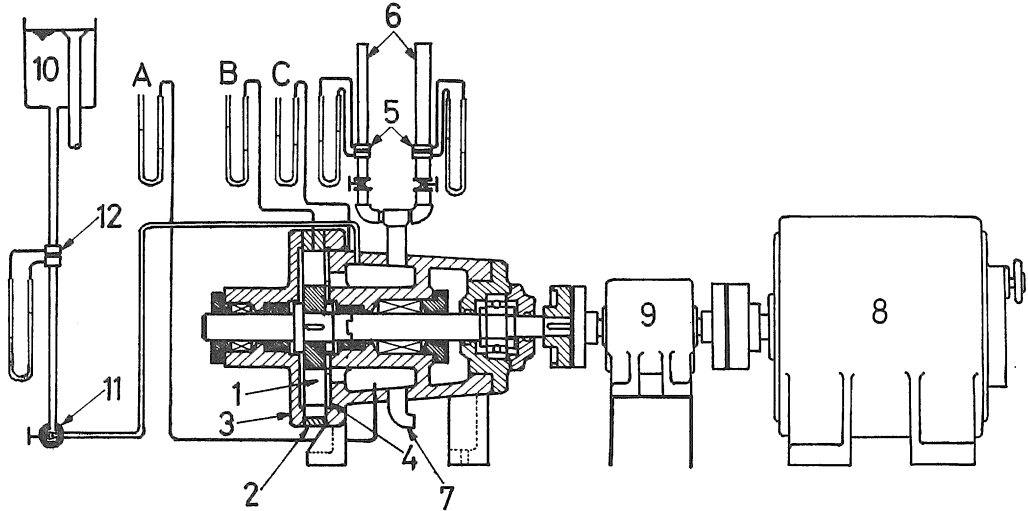


Fig. 1. General view of the experimental apparatus.

1: Runner 2: Elmo type casing 3: Casing cover 4: Side plate 5: Gas flow meter  
 6: Suction pipe 7: Discharge pipe for piston water 8: Variable speed motor 9: Wire strain gauge torque-meter 10: Feed tank for supply water 11: Needle valve 12: Flow meter for supply water  
 A: Degree of vacuum B: Pressure on the wall surface of casing C: Pressure at the tip of runner

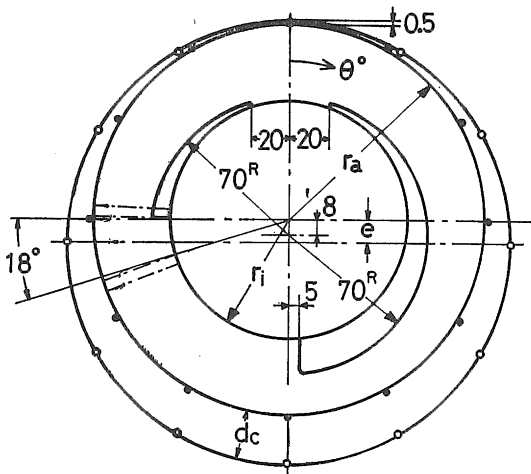


Fig. 2. Details of the suction and the exhaust port and the measured positions of various pressures.  
 Solid circle: measured position of pressure at the tip of runner.  
 Hollow circle: measured position of pressure on the wall surface of casing.  
 e: eccentricity rate of casing.

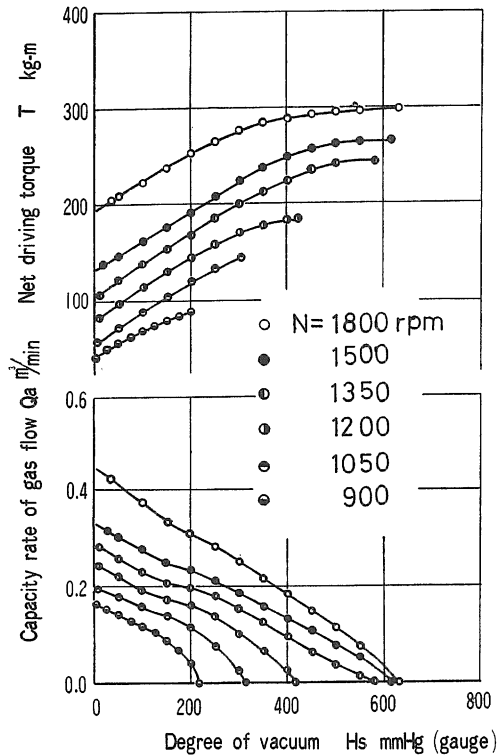


Fig. 3. Net driving torque and capacity rate of gas flow vs. degree of vacuum, ( $E = 0.12$ )

3. For the purpose of determining a mechanical loss we measured the driving torques of the pump while discharging gradually the piston water. And the minimum driving torque was considered as a mechanical loss.

The pressure in the hollow space of runner\*\*\*\* was measured with a semiconductor pressure transducer attached to the inside of the pump shaft.

In order to investigate the flow state of piston water, we replaced the casing cover made of iron cast with one of transparent synthetic resin and took a photograph with a stroboscope.

### 3. Experimental Results and Discussion

#### 3. 1. Characteristic curve

Fig. 3 shows the characteristic curves of this pump in case of the eccentricity (E) of 0.12 as a concrete example that pump performance varies with the number of revolutions of the runner (N). Where,  $H_s$  is the degree of vacuum,  $Q_a$  the capacity rate of gas flow measured in the atmosphere pressure, and  $T$  the net driving torque.

In Fig. 4, the dimensionless characteristic curves are shown in order to examine the similar relations of this pump. (The measured values are partially omitted due to the intricacy of drawing.) Assuming that the characteristic curves depend mainly on the flow state of piston water, each dimensionless quantity in this figure was defined as follows :

$$H_{so} = \frac{(H_s/760) \times 10.33}{U^2/2g}$$

$$Q_{so} = \frac{Q_a \times 760 / (760 - H_s)}{U d_c b_c}$$

$$L_0 = \frac{T\omega}{\gamma/g U^3 d_c b_c}$$

where

$U$  = peripheral velocity of the runner

$b_c$  = effective width of the casing

$d_c$  = depth of the crescent shaped passage of the casing at the shut-off position of suction port (refer to Fig. 2)

\*\*\*\* This is the space which is surrounded by the free surface of piston water and the hub of runner.

$\omega$  = angular velocity of the runner

$\gamma/g$  = specific mass of piston water

As is obvious from Fig. 4, the curves ( $H_{so} - L_0$ ) roughly overlap except for the lower speed of revolutions than  $N = 1000$  rpm for all the eccentricities. This result make it clear that the piston water compresses the gas in the hollow space of runner but its compression work is far less than the work requested to circulate the piston water : The runner does not directly exert work to the gas and a part of the work done on the piston water is used to compress the gas. Accordingly, it is sufficient to consider only the work done on the piston water as pump input. On the contrary, the aforementioned law of similarity does not extremely hold for the curve ( $H_{so} - Q_{so}$ ). This may be partly because the thickness of piston water layer at the shut-off position of suction port changes with N. A detailed discussion about the boundary surface of gas and piston water are found later.

And now the curves ( $H_{so} - Q_{so}$ ) or ( $H_s - Q_a$ ) have a remarkable feature as compared with them in case of Nash type casing : The decreasing tendency of  $Q_{so}$  or  $Q_a$  is different before and after the singular point decided every number of revolution. Up to the present this feature seems to have been overlooked as the internal leakage of the pump or the experimental error, but may be suggested to be caused by the transformation of the boundary surface of gas and piston water. Its ground is given as under.

Fig. 5 shows the state that three kinds of pressures in the interior of the pump change with  $H_s$  in the neighbourhood of the end of compression range ( $\theta = 240^\circ$  in Fig. 2) : pressure in the hollow space of runner ; pressure at the tip of runner ; pressure difference between them. Taking only the centrifugal force of piston water into account, the thickness of piston water layer is approximately in proportion to the pressure difference. As can readily be seen from Fig. 5, the pressure difference changes discontinuously at the singular point. It can be approved, therefore, that the shape of the boundary surface of gas and piston water transforms rapidly at the singular point ; in other words, the shape of the boundary surface is converted into a new

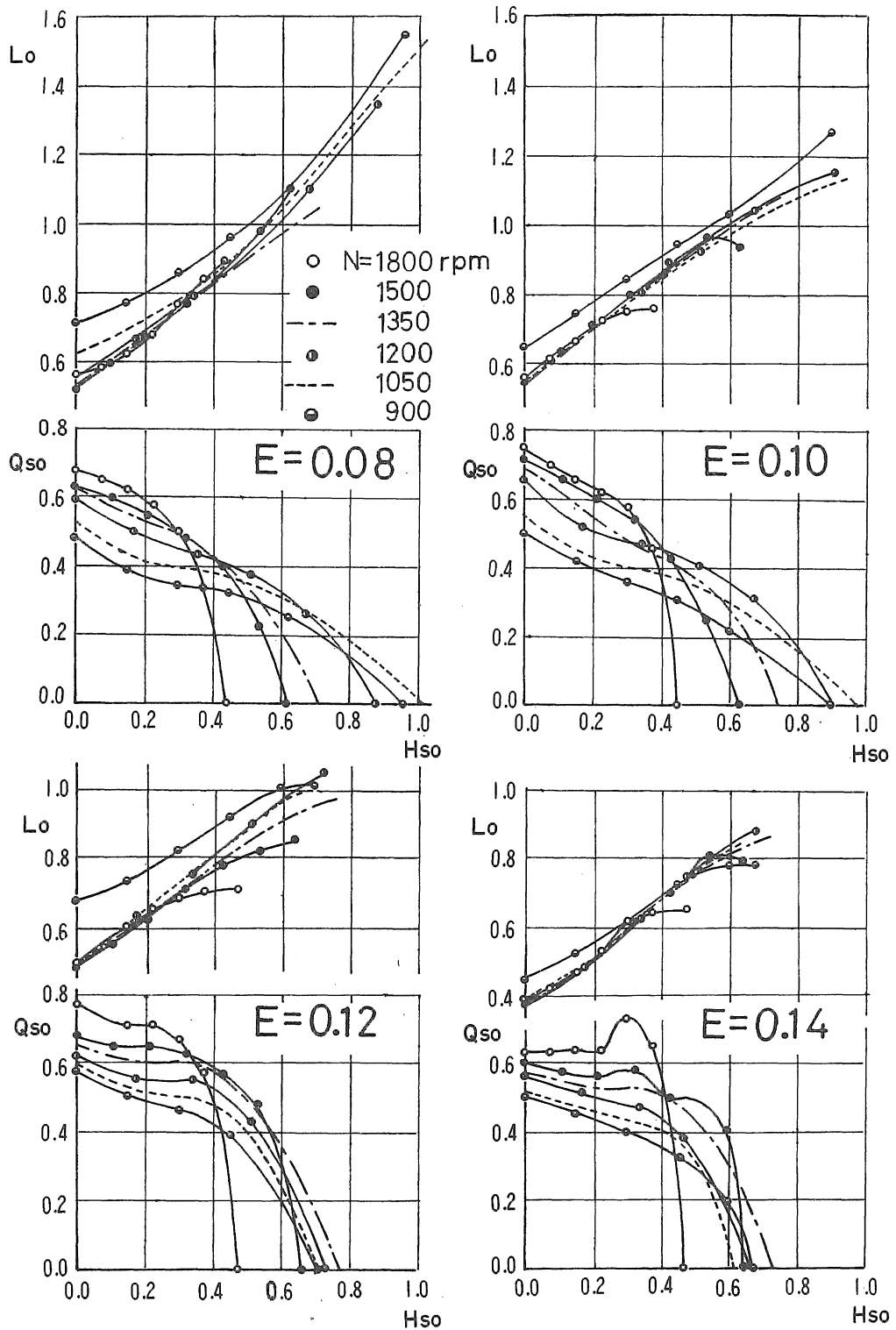


Fig. 4. Dimensionless characteristic curve.

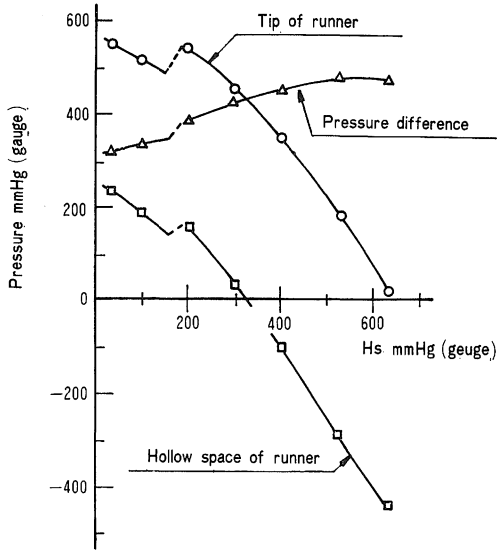
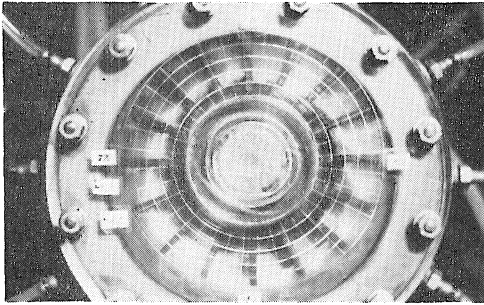


Fig. 5. Pressure in the interior of the pump vs. degree of vacuum, at  $\theta = 240^\circ$ . ( $E = 0.12$ ,  $N = 1800$  rpm)

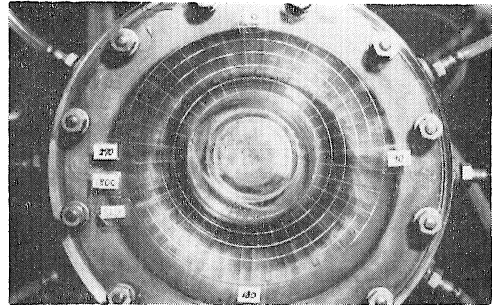
one by reason of the energy unbalance between the gas and the piston water in the neighbourhood of the end of compression range.

### 3. 2. Shape of the boundary surface of gas and piston water

Fig. 6 is an example of the photographs which illustrate the flow state of piston water. In order to investigate the shape of the boundary surface of gas and piston water, it was read from such photographs. (It was difficult, however, to read definitely because the boundary surface was partially foggy.) The examples of photographical measurements are drawn in Fig. 7. In this figure  $R$  as an ordinate is the dimensionless quantity divided the radial distance between the center of runner and the boundary surface by  $r_a$  and an arrow indicates the position of the maximum  $R$ . The following tendencies became clear after examining the results of photog-



Synchronous photo.



Asynchronous photo.

Fig. 6. Photograph showing the flow state of gas flow. ( $E = 0.12$ ,  $N = 1800$  rpm,  $H_s = 630$  mmHg (gauge))

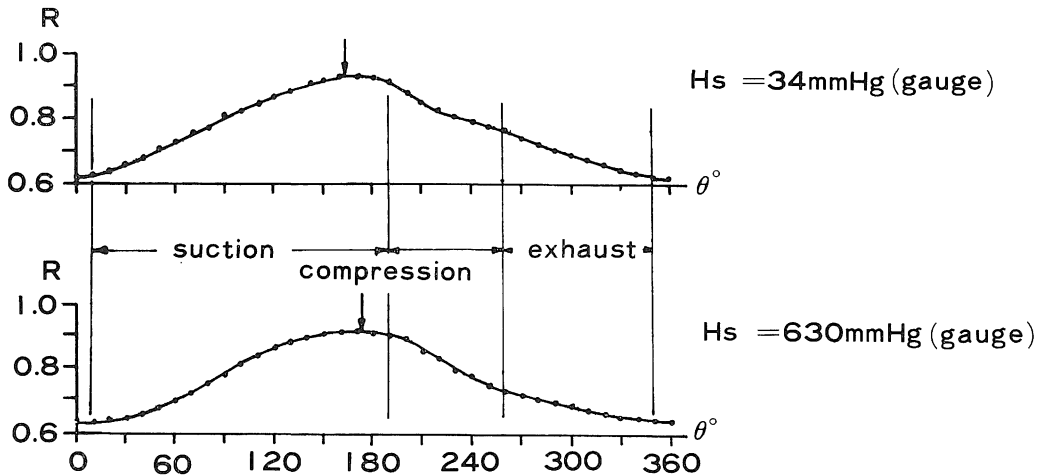


Fig. 7. Shape of the boundary surface of gas and piston water. ( $E = 0.12$ ,  $N = 1800$  rpm)  $R$ : dimensionless quantity divided the radial distance between the center of runner and the boundary surface by  $r_a$ .

raphical measurements : (a) The boundary surface does not contact with the hub of runner at the top of casing ( $\theta = 0^\circ$ ) and its clearance increases with the increase of  $H_s$ . (b) The position of the maximum  $R$  moves to the direction of compression range as  $H_s$  increases.

### 3. 3. Maximum degree of vacuum

The maximum degree of vacuum ( $H_{s,max}$ ) is plotted as an ordinate with the number of revolutions of the runner ( $N$ ) as an abscissa in Fig. 8. Fig. 8 reveals that a transitional point exists on all the curves ( $N-H_{s,max}$ ) and the increasing tendency of  $H_{s,max}$  divides into two types near its point; hence, the experimental curves do not agree even qualitatively to the curve obtained from Pfleiderer's formula (dotted line in this figure).

Under the higher speed of revolution than the transitional point, the increasing grade of  $H_{s,max}$  is very gradual and that the driving state of the pump is greatly stable. These facts are from the following reason: The gas returns from exhaust range to suction one through the aforementioned clearance at the top of casing; then, its leakage rate of gas flow becomes equal to the capacity rate of gas flow compressed in compression range.

On the other hand, under the lower speed of revolution,  $H_{s,max}$  increases in approximate proportion to the second power of  $N$  for all the eccentricities. But it is difficult to keep

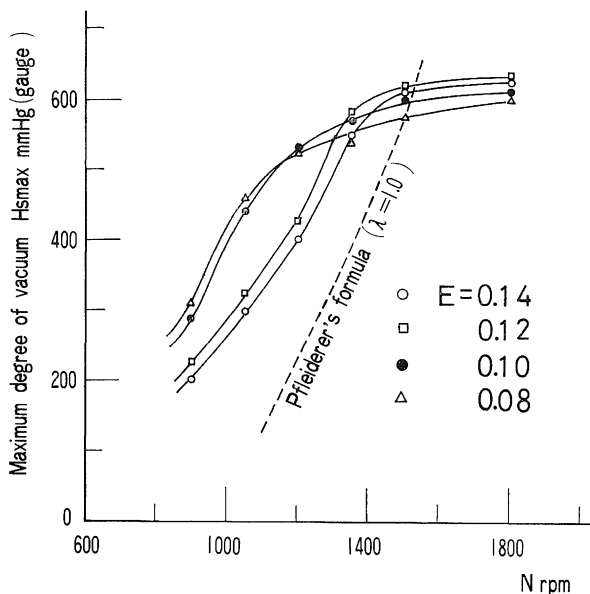


Fig. 8. Maximum degree of vacuum vs. number of revolutions of the runner.

the pump in motion for a long time because the energy balance of piston water is destroyed and the greater part of piston water is discharged out of the pump at a once. According to the observation of piston water flow in case of shutting the suction valves, this instability seems to be caused by the fact that the piston water in the crescent shaped passage of the casing stagnates just before the opening position of exhaust port.

Now, the maximum value of  $H_{s,max}$  for each eccentricity was almost the same as that in Nash type casing; so far as the present experiments are concerned, we could not find the special evidence that Elmo type casing was more favourable as a high vacuum pump than Nash type casing.

### 3. 4. Iso-efficiency curve

Each of Fig. 9 illustrates the iso-efficiency curves based on the assumption that the gas isothermally experiences volume change. The values of the best efficiency increase as the eccentricity ( $E$ ) increases, though there is not very much difference between  $E = 0.12$  and  $0.14$ . A dotted line drawn in Fig. 9 designates the number of revolutions of the runner ( $N$ ) which gives the best efficiency at each degree of vacuum ( $H_s$ ) and a chain line does  $H_s$  at the best efficiency point in case of driving the pump under  $N = \text{constant}$ .

Both the shape and the value of the iso-efficiency curve were inferior to those in Nash type casing just as we had anticipated.

## 4. Conclusions

The results obtained from the experiments on the wet vacuum pump with Elmo type casing are summarized as follows:

- (1) The low of similarity for the capacity rate of gas flow is closely related to the shape of the boundary surface of gas and piston water.
- (2) The various characteristic curves of Elmo type casing almost have the same tendency as those of Nash type casing, but a singular phenomenon occurs in regard to the capacity rate of gas flow. This phenomenon can be qualitatively interpreted by the fact that the boundary surface of gas and piston water changes delicately on account of the energy unbalance between the gas and the piston water.
- (3) Although it has been generally said that

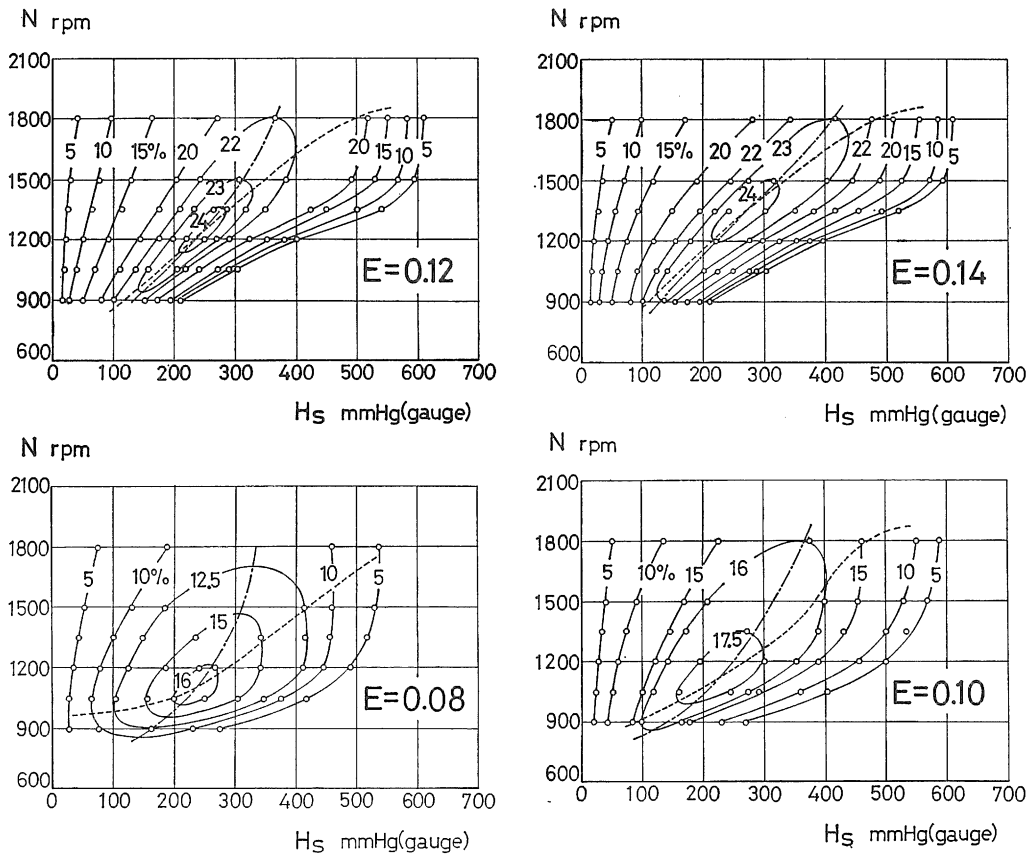


Fig. 9. Iso-efficiency curve obtained for isothermal change.

Elmo type casing is superior to Nash type casing as a high vacuum pump in view of the longer compression range in the former, it is not always true.

(4) A transitional point exists on the curve showing the relation between the maximum degree of vacuum and the number of revolutions of the runner; consequently, the tendency of the curve calculated with Pfleiderer's formula scarcely agrees to the experimental results.

The limit of vacuum at the high speed of revolution is due to the clearance between the hub of runner and the boundary surface of gas and piston water at the top of casing.

(5) Concluding synthetically according to the capacity rate of gas flow, the degree of vacuum, the iso-efficiency curve, etc., the optimum eccentricity of Elmo type casing may be the order of  $E = 0.12$ .

**ACKNOWLEDGEMENT:** The authors are indebted to Mr. T. Hibino, Mr. A. Hiraishi, Mr. Y. Ueda, Mr. T. Sakoda, and other graduates of Osaka Pref. University for gener-

ous assistance in the course of these experiments.

#### References

- 1) C. Pfleiderer: Die Kreiselpumpen, 4 Aufl., Springer-Verlag, p. 555-571 (1955).
- 2) O. Torii: Proc. of JSME., 710-8, p. 49-52(1971).
- 3) Y. Senoo and T. Sasai: Trans. of JSME., **26**, 162, p. 217-223 (1960).
- 4) O. Torii: Trans. of JSME., **30**, 213, p. 599-606 (1964).